Extended Experimental Procedures:

Isolation of renal tubules and cells:

C57BL-6 mice (4-6 weeks old, 15–20 g body weight; Charles River, l'Arbresle, France) were anesthetized using Xylacine (Rompun®) 8 mg/kg and Ketamine 1000 (Virbac) 80 mg/kg. Kidneys were perfused via the heart with 15 ml of L-15 Leibovitz medium (Sigma, Saint Quentin Fallavier, France) supplemented with collagenase (CLS II, Worthington; 300 U/ml) and removed, as previously described [1]. Small pieces of cortex were incubated at 37°C for 20–50 min in the same collagenase-containing medium, rinsed, and kept at 4°C. Tubular fragments were dissected-out under a stereomicroscope just before use and transferred to a petri dish placed on the stage of an inverted microscope (Axiovert 40, Zeiss) for patch recordings.

Isolation, immortalization and culture of mouse PCT cells:

5-6 weeks old C57Bl/6 mice were used. Proximal convoluted tubules were microdissected under sterile conditions. Kidneys were perfused with Hanks' solution (GIBCO) containing 700 kU/l collagenase (Worthington), cut into small pyramids that were incubated for 1 h at room temperature in the perfusion buffer (160 kU/l collagenase, 1 % Nuserum, and 1 mM $CaCl_2$), and continuously aerated. The pyramids were then rinsed thoroughly in the same buffer devoid of collagenase. The individual nephrons were dissected by hand in this buffer under binoculars using stainless steel needles mounted on Pasteur pipettes. PCT corresponded to the 1- to 1.5-mm segment of tissue located immediately after the glomerulus. Tubules were rinsed in the dissecting medium and transferred to collagen-coated 35-mm petri dishes filled with culture medium composed of equal quantities of DMEM and Ham's F-12 (GIBCO) containing 15 mM $NaHCO_3$, 20 mM HEPES, pH 7.4, 1 % serum, 2 mM glutamine, 5 mg/l insulin, 50 nM dexamethasone, 10 µg/l epidermal growth factor, 5 mg/l transferrin, 30 nM sodium selenite, and 10 nM triiodo-L-thyronine. Cultures were maintained at 37 °C in a 5 % CO_2-95 % air water-saturated atmosphere. The medium was renewed 4 days after seeding and then every 2 days. 10-day-old primary cultures of mouse proximal tubules were transfected with pSV3 *neo* using Lipofectin (Invitrogen). After 48 h, selection of the clones was performed by the addition of G418 (500 µg/ml). Resistant clones were isolated, subcultured, and used after 10 trypsinization steps. Immortalized proximal cell (PCT) lines were grown on collagen-coated supports (35-mm Petri dishes) in a 5 % CO_2 atmosphere at 37 °C in the culture medium described above.

Co-immunoprecipitation experiments:

COS cells were seeded at $1X10^6$ in 60 mm plates the day before transfection. Cells were transfected using the DEAE Dextran technique. Piezo constructs were all transfected at 5 µg /plate while the other constructs were transfected as follows: MYC-PC2ΔN203 5 µg, MYC-PC2 4 µg, MYC-PC2-740X 4 µg, MYC-PC2-701X 1 µg, MYC-PC2-690X 1 µg, MYC-Kv9.3 5 µg, MYC-Kv2.1 0.5 µg. The immunoprecipitation was performed 72h later. Cells were washed 1X with PBS- then lysed in a buffer containing: 150 mM NaCl, 10 mM Tris pH7.4, 1 mM EDTA, 1 mM EGTA, 1 % Triton-X 100, 0.5 % NP40, Complete protease inhibitors (Roche), Phosphatase inhibitors (Sigma), Pefabloc SC plus (Roche). Lysates were sonicated then rotated at 4°C for 30 minutes. They were then centrifuged at 14,000 rpm for 5 mins and 60 µl removed for inputs. The rest of the supernatants were precleared with 25 µl of protein

G magnabeads (NEB) for 30 minutes rotating at 4°C. 500 µl was removed, brought up to 1 ml with lysis buffer and incubated with 25 µl of protein G magnabeads chemically crosslinked with 1 µg of antibody 3F10 (Roche). Samples were rotated at 4°C for 1 hour. The beads were then stringently washed 3Xs with vortexing and 1 ml of lysis buffer containing 250 mM NaCl. The last drops of liquid were removed and 25 µl of 0.1 M glycine was added to elute the immunoprecipitate. Samples were vortexed for 5 mins at RT and the supernatants transferred to tubes containing 5 µl of 1M Tris pH 7.5 and 6 µl of loading buffer. Samples were heated for 10 mins at 70°C and then charged on a criterion 4-15% TGX gel (BIO-RAD). The gel was transferred to PVDF (Perkin Elmer) using a Tris glycine buffer containing 20% methanol. After blocking for 1 hr in PBS- / 0.1% Tween / 5% milk. The top of the membranes (cut between 250 and 130 kDa) were incubated with a 1:1000 dilution of 3F10 and the bottom incubated with a 1:1000 dilution of 9E10 (Roche) overnight. After washing several times in PBS- / 0.1% Tween, the blots were incubated with a 1:30,000 dilution of anti rat-HRP or anti mouse HRP for 1 hr. The blots were then washed as before and developed with Western lightening Ultra (Perkin Elmer). Blots were imaged using a LAS imager.

Confocal imaging:

PCT cells were co-transfected with a Piezo1-EGFP fusion, either with a mock DsRed expression vector, or together with PC2 or PC2-740X ires2 DsRed plasmid (0.8 µg in total). The SAC activity of Piezo1-EGFP was verified in transfected COS cells and was identical to the untagged Piezo1 construct. Living cells were visualized 24-48 hrs after transfection by confocal fluorescence microscopy (Leica SP5). The quantitative analysis of Piezo1 expression at the plasma membrane was done using the image J software (Rasband, W.S., ImageJ, U. S. National Institutes of Health, Bethesda, Maryland, USA, http://imagej.nih.gov/ij/, 1997-2012.). A mask corresponding to the whole cell area (EGFP signal) minus the cytosolic area (DsRed signal) was created for each cell and intensity of the Piezo1-EGFP signal at the plasma membrane was quantified.

In additional experiments, plasma membrane of living PCT cells was labeled by the addition of wheat germ agglutinin (WGA; W11262, Molecular Probes) at 3 µg/ml.

Native PC2 was visualized in PFA-fixed PCT cells using the E-20 antibody (Santa Cruz Biotechnology sc-10377).

Animals:

All experiments were performed according to policies on the care and use of laboratory animals of European Community Legislation. The study was approved by the local Committee for ethical and safety issues (CIEPAL-Azur). All efforts were made to minimize animal suffering and reduce the number of animals used. The animals housed under controlled laboratory conditions with a 12-h dark–light cycle, a temperature of 21 ± 2 °C, and a humidity of 60–70 % had free access to standard rodent diet and tap water.

Electrophysiology:

The experiments were carried out at room temperature. Currents were filtered at 1 kHz, digitized at 10 kHz, and analyzed with pCLAMP9.2 (Axon Instruments) and ORIGIN8.5 (Microcal, Northampton, MA) softwares. Pressure effect curves were fitted with a Boltzmann function ($I = \frac{I1-I2}{1+e^{(P-P0.5)/k}}+I2$). SAC currents kinetics were fitted with a standard exponential function + a constant current I_C at a pressure value of -50 mm Hg. Single channel analysis was performed with the Single Channel Detection and Analysis mode of

pCLAMP9.2 (Axon Instruments). Open channel probability was determined by amplitude histogram analysis in patches with less than 3 active channels (Po=I/N*i).

Statistical analysis:

Peak currents were measured and significance of the differences was tested with a permutation test (R Development Core Team: http://www.r-project.org/) ($n < 30$) or two samples t Test ($n > 30$). One star indicates $p < 0.05$, two stars $p < 0.01$ and three stars $p < 0.001$. Data represent mean ± standard error of the mean. The number of independent times each experiment has been repeated (n) is indicated throughout the manuscript and is shown in figures.

Legends of Supplementary figures:

Figure Supp 1: Piezo1 knock-down in cultured PCT cells.
Normalized QPCR expression of *Piezo1*, *Piezo2*, *Pkd1*, *Pkd2*, *TRP* channels, in either siNT or si1Piezo1- (shown in a; n=3) or si2Piezo1-transfected PCT cells (shown in b; n=3). c) Western blot demonstrating that native PC2 expression in PCT cells is not altered upon Piezo1 knockdown by si1Piezo1 or si2Piezo1. QPCR experiments indicated that the knock-down of Piezo1 was 64% and 66% for si1Piezo1 and si2Piezo1, respectively. d) The subcellular localization of PC2 is not altered in PCT cells upon Piezo1 knockdown by si1Piezo1 or si2Piezo1. PC2 is visualized in red and the nuclei are labeled in blue by Hoechst staining.

Figure Supp 2: Single channel current amplitude and open channel probability of SACs is not influenced by PC2-740X.
a) Single channel current amplitude measured at a holding potential of -80 mV for native SACs in PCT cells, either in the absence (empty bar; mock) or in the presence of PC2-740X (red bar). b) Open probability of SACs recorded in PCT cells transfected either with a mock (empty bar) plasmid or with PC2-740X (red bar) at a pressure value of -40 mm Hg and a holding potential of -80 mV. Number of patches analyzed are indicated near each histogram bar.

Figure Supp 3: Piezo1 and Piezo2 mRNA expression is not altered by PC2-740X.
QPCR expression of Piezo1 and Piezo2, normalized to TOP1 expression, in PCT cells overexpressing either TRPC1 or PC2-740X (as indicated). Krustal-Wallis test was used to compare mock, +TRPC1 and +PC2-740X.

Figure Supp 4: Native and exogenous Piezo1 expression in PCT and COS-7 cells.
a) Mean cell-attached native SACs current at a holding potential of -80 mV in mock-transfected PCT cells (n = 16). b) Mean (n = 22) cell-attached exogenous Piezo1 current at a holding potential of -80 mV in Piezo1-transfected PCT cells. The mean native SAC current (panel a) was digitally subtracted from the global current (native SACs + Piezo1) illustrated in Fig. 4a. c) Top trace: Mean (n = 19) cell-attached native SAC current at a holding potential of -80 mV in mock-transfected COS-7 cells. d) Mean (n = 32) cell-attached exogenous Piezo1 currents at a holding potential of -80 mV in transfected COS-7 cells. The mean native SAC current (panel c) was digitally subtracted from the global current (native SACs + Piezo1) illustrated in Fig. 4a. Bottom traces illustrate the pressure pulses.

Figure Supp 5: **Reversal potential of exogenous Piezo1 expressed in PCT cells.**
Typical example of a cell-attached Piezo1 current in a transfected PCT cell recorded at a holding potential of -80 mV (top trace) or 0 mV (middle trace). Lower trace illustrates the pressure pulses.

Figure Supp 6: Piezo1 plasma membrane expression is not altered by PC2 or PC2-740X.
a) Representative overlay image of Piezo1-EGFP expression (in green) in transfected PCT cells together with a DsRed ires DsRed expression vector (in red), visualized by confocal microscopy. b) Piezo1-EGFP together with PC2 ires DsRed. c) Piezo-1-EGFP together with PC2-740X ires DsRed. The scale bar is 3 μm. d) Quantification of Piezo1 expression at the plasma membrane (mean intensity in arbitrary units). Numbers of analyzed cells are indicated.

Figure Supp 7: Expression of Piezo1-EGFP at the plasma membrane of transiently transfected PCT cells.
a-c) Confocal imaging of living PCT cells transfected with Piezo1-EGFP (in green; first panels) and labeled with WGA (in red, second panels). The merge image is shown (third panels). The scale bar is 3 μm.

Figure Supp 8: Co-immunoprecipitation of PC2 with Piezo1.
PC2 (or -740X) is immunoprecipitated with an anti MYC antibody and Piezo1 is revealed with an anti HA antibody. EGFP is used as a negative control.

Figure Supp 9: Localization of Piezo1-EGFP and mCherry-PC2 or mCherry-PC2-740X in transiently transfected PCT cells.
a-c) Confocal imaging of living PCT cells transfected with Piezo1-EGFP (in green; first panel) and mCherry-PC2 (in red, second panel). The merged image is shown (third panel). d-f) Expression of Piezo1-EGFP (in green; first panel) together with mCherry-PC2-740X (in red; second panel) in PCT living transfected cells. The merged image is shown (third panel). The scale bar is 3 μm.

Extended discussion:

A key finding of our study is that Piezo1 is critically required for non-selective SAC activity in renal PCT epithelial cells. Moreover, as previously reported, overexpression of Piezo1 significantly increased SAC activity in transfected cells [2, 3]. Both Piezo1 and native SACs in PCT cells reverse at about 0 mV and are blocked by ruthenium red (although a non-specific inhibitor) and by the spider venom peptide GsMTx-4 [3-6]. These findings, along with the recent demonstration that Piezos are pore forming subunits in artificial bilayers (although not shown to be mechano-sensitive upon reconstitution) [4], are consistent with the possibility that Piezo1 encodes the non-selective SACs in renal tubular epithelial cells.

SACs are functional at the basolateral side of isolated kidney PCT. Since we were unable to obtain gigaseals at the apical side, the possible presence of these mechano-sensitive channels at this level, including the brush border and/or the primary cilium, cannot be ruled out. Native SACs from tubular epithelial cells were characterized by fast activation, lack of inactivation and a remarkably slow deactivation. By contrast, heterologous expression of Piezo1 in PCT or COS-7 cells, or as previously demonstrated in HEK cells [2], consistently

resulted in SAC currents with a prominent inactivation and a fast deactivation. However, native SACs in PCT cells were critically dependent on Piezo1, as determined by a knock-down strategy. These findings suggest that the kinetics of native SACs in tubular epithelial cells may be dependent on regulatory elements affecting Piezo1 activity, but which would be limited as Piezo1 overexpression always resulted in a fast inactivating and deactivating exogenous SAC current, even in PCT cells. Another possibility is that a Piezo1 splice variant(s) in PCT cells may encode a SAC lacking inactivation and with a slow deactivation, however such variant(s) have not yet been identified. Inactivation or adaptation of mechano-gated ion channels is of importance for the role of such channels in mechanosensory specialized cells such as hair cells or touch receptors [7-13]. However, in non-specialized cells, fast inactivation of SACs would not be consistent with slow and steady pressure changes, as those occuring for instance in the kidney [14-21]. Inactivation and/or deactivation mechanisms of SACs may be independent of the channel itself, but instead could be linked to the cytoskeleton [22, 23].

Importantly, the inhibitory effect of PC2 and PC2-740X was not related to an effect on Piezo1 transcription, protein expression or trafficking to the plasma membrane. Whether PC2 may form a heteromultimer with and inhibit Piezo1 (demonstrated to be a tetramer [4]), or whether it may act as a regulatory inhibitory auxillary β subunit will need to await further investigations.

Most of WT PC2 is seen at the level of the ER [24]. However, a small fraction of PC2 can be detected at the plasma membrane and could be sufficient for Piezo1 inhibition [25-27]. Alternatively, PC2 at the ER may influence Piezo1 at the cell surface when both membranes come in close contact. This functional interaction may possibly involve an intermediate element, such as the PC2 interactor filamin A which is required for the regulation of the stretch-sensitive TREK-2 K_{2P} channels by PC2 [25].

It was previously demonstrated in elegant studies that polycystins are required for flow sensing by the primary cilium in renal epithelial, endothelial or nodal cells [28-32]. The postulate is that PC1 (or an isoform in nodal cells) may act as the flow sensor which in turn would control opening of the associated calcium-permeable channel PC2 [for reviews33, 34]. Whether native Piezo1 is located at the level of the primary cilium in renal tubular cells is currently unknown and would require a specific antibody which is unfortunately not yet available. The role of Piezo1 in flow sensing by the primary cilium needs to be investigated in future studies. In addition to experiencing shear stress associated with intraluminal urine flow, tubular cells are also physiologically exposed to stretch [35]. For instance, collecting duct cells are rhythmically distended when a bolus of urine is pushed through by pelvic peristaltism [36]. Upstream renal tubules may also be affected by back propagation of this pressure wave [36]. Further studies of the physiological role of Piezo1 in the kidney will need to await for the availability of a Piezo1 knockout mouse model.

References:

1. Lourdel S, Paulais M, Marvao P, Nissant A, Teulon J (2003) A chloride channel at the basolateral membrane of the distal-convoluted tubule: a candidate ClC-K channel. *J Gen Physiol* 121: 287-300

2. Coste B, Mathur J, Schmidt M, Earley TJ, Ranade S, Petrus MJ, Dubin AE, Patapoutian A (2010) Piezo1 and Piezo2 are essential components of distinct mechanically activated cation channels. *Science* 330: 55-60
3. Bae C, Sachs F, Gottlieb PA (2011) The mechanosensitive ion channel Piezo1 is inhibited by the peptide GsMTx4. *Biochemistry* 50: 6295-6300
4. Coste B *et al* (2012) Piezo proteins are pore-forming subunits of mechanically activated channels. *Nature* 483: 176-181
5. Suchyna TM, Johnson JH, Hamer K, Leykam JF, Gage DA, Clemo HF, Baumgarten CM, Sachs F (2000) Identification of a peptide toxin from Grammostola spatulata spider venom that blocks cation-selective stretch-activated channels. *J Gen Physiol* 115: 583-598
6. Suchyna TM, Tape SE, Koeppe RE, 2nd, Andersen OS, Sachs F, Gottlieb PA (2004) Bilayer-dependent inhibition of mechanosensitive channels by neuroactive peptide enantiomers. *Nature* 430: 235-240
7. Chalfie M (2009) Neurosensory mechanotransduction. *Nat Rev Mol Cell Biol* 10: 44-52
8. Kung C (2005) A possible unifying principle for mechanosensation. *Nature* 436: 647-654
9. Gillespie PG, Walker RG (2001) Molecular basis of mechanosensory transduction. *Nature* 413: 194-202
10. Nilius B, Honore E (2012) Sensing pressure with ion channels. *Trends Neurosci* 35: 477-486
11. Delmas P, Hao J, Rodat-Despoix L (2011) Molecular mechanisms of mechanotransduction in mammalian sensory neurons. *Nat Rev Neurosci* 12: 139-153
12. Wood JN, Eijkelkamp N (2012) Noxious mechanosensation - molecules and circuits. *Curr Opin Pharmacol* 12: 4-8
13. Smith ES, Lewin GR (2009) Nociceptors: a phylogenetic view. *J Comp Physiol A Neuroethol Sens Neural Behav Physiol* 195: 1089-1106
14. Quinlan MR, Docherty NG, Watson RW, Fitzpatrick JM (2008) Exploring mechanisms involved in renal tubular sensing of mechanical stretch following ureteric obstruction. *Am J Physiol Renal Physiol* 295: F1-F11
15. Rohatgi R, Flores D (2010) Intratubular hydrodynamic forces influence tubulointerstitial fibrosis in the kidney. *Curr Opin Nephrol Hypertens* 19: 65-71
16. Wyker AT, Ritter RC, Marion D, Gillenwater JY (1981) Mechanical factors and tissue stresses in chronic hydronephrosis. *Invest Urol* 18: 430-436
17. Power RE, Doyle BT, Higgins D, Brady HR, Fitzpatrick JM, Watson RW (2004) Mechanical deformation induced apoptosis in human proximal renal tubular epithelial cells is caspase dependent. *J Urol* 171: 457-461
18. Cachat F, Lange-Sperandio B, Chang AY, Kiley SC, Thornhill BA, Forbes MS, Chevalier RL (2003) Ureteral obstruction in neonatal mice elicits segment-specific tubular cell responses leading to nephron loss. *Kidney Int* 63: 564-575
19. Praetorius HA, Frokiaer J, Leipziger J (2009) Transepithelial pressure pulses induce nucleotide release in polarized MDCK cells. *Am J Physiol Renal Physiol* 288: 133-141
20. Derezic D, Cecuk L (1982) Hydrostatic pressure within renal cysts. *Br J Urol* 54: 93-94
21. Tanner GA, McQuillan PF, Maxwell MR, Keck JK, McAteer JA (1995) An in vitro test of the cell stretch-proliferation hypothesis of renal cyst enlargement. *J Am Soc Nephrol* 6: 1230-1241
22. Sachs F, Morris CE (1998) Mechanosensitive ion channels in nonspecialized cells. *Rev Physiol Biochem Pharmacol* 132: 1-77

23. Gottlieb PA, Bae C, Sachs F (2012) Gating the mechanical channel Piezo1: A comparison between whole-cell and patch recording. *Channels (Austin)* 6: 282-289
24. Koulen P, Cai Y, Geng L, Maeda Y, Nishimura S, Witzgall R, Ehrlich BE, Somlo S (2002) Polycystin-2 is an intracellular calcium release channel. *Nat Cell Biol* 4: 191-197
25. Peyronnet R *et al* (2012) Mechanoprotection by Polycystins against Apoptosis Is Mediated through the Opening of Stretch-Activated K(2P) Channels. *Cell Rep* 1: 241-250
26. Bai C, Giamarchi A, Rodat-Despoix L, Padilla F, Downs T, Tsiokas L, Delmas P (2008) Formation of a novel receptor-operated channel by heteromeric assembly of TRPP2 and TRPC1 subunits. *EMBO Rep* 9: 472-479
27. Bai CX, Kim S, Li WP, Streets AJ, Ong AC, Tsiokas L (2008) Activation of TRPP2 through mDia1-dependent voltage gating. *Embo J* 27: 1345-1356
28. Aboualaiwi WA, Takahashi M, Mell BR, Jones TJ, Ratnam S, Kolb RJ, Nauli SM (2009) Ciliary Polycystin-2 Is a Mechanosensitive Calcium Channel Involved in Nitric Oxide Signaling Cascades. *Circ Res* 104: 860-869
29. Nauli SM *et al* (2003) Polycystins 1 and 2 mediate mechanosensation in the primary cilium of kidney cells. *Nat Genet* 33: 129-137
30. Nauli SM, Kawanabe Y, Kaminski JJ, Pearce WJ, Ingber DE, Zhou J (2008) Endothelial cilia are fluid shear sensors that regulate calcium signaling and nitric oxide production through polycystin-1. *Circulation* 117: 1161-1171
31. Pennekamp P, Karcher C, Fischer A, Schweickert A, Skryabin B, Horst J, Blum M, Dworniczak B (2002) The ion channel polycystin-2 is required for left-right axis determination in mice. *Curr Biol* 12: 938-943
32. Yoshiba S *et al* (2012) Cilia at the Node of Mouse Embryos Sense Fluid Flow for Left-Right Determination via Pkd2. *Science* 338: 226-231
33. Nauli SM, Zhou J (2004) Polycystins and mechanosensation in renal and nodal cilia. *Bioessays* 26: 844-856
34. Delmas P (2004) Polycystins: from mechanosensation to gene regulation. *Cell* 118: 145-148
35. Patel A, Honore E (2010) Polycystins and renovascular mechanosensory transduction. *Nat Rev Nephrol* 6: 530-538
36. Dwyer TM, Schmidt-Nielsen B (2003) The renal pelvis: machinery that concentrates urine in the papilla. *News Physiol Sci* 18: 1-6

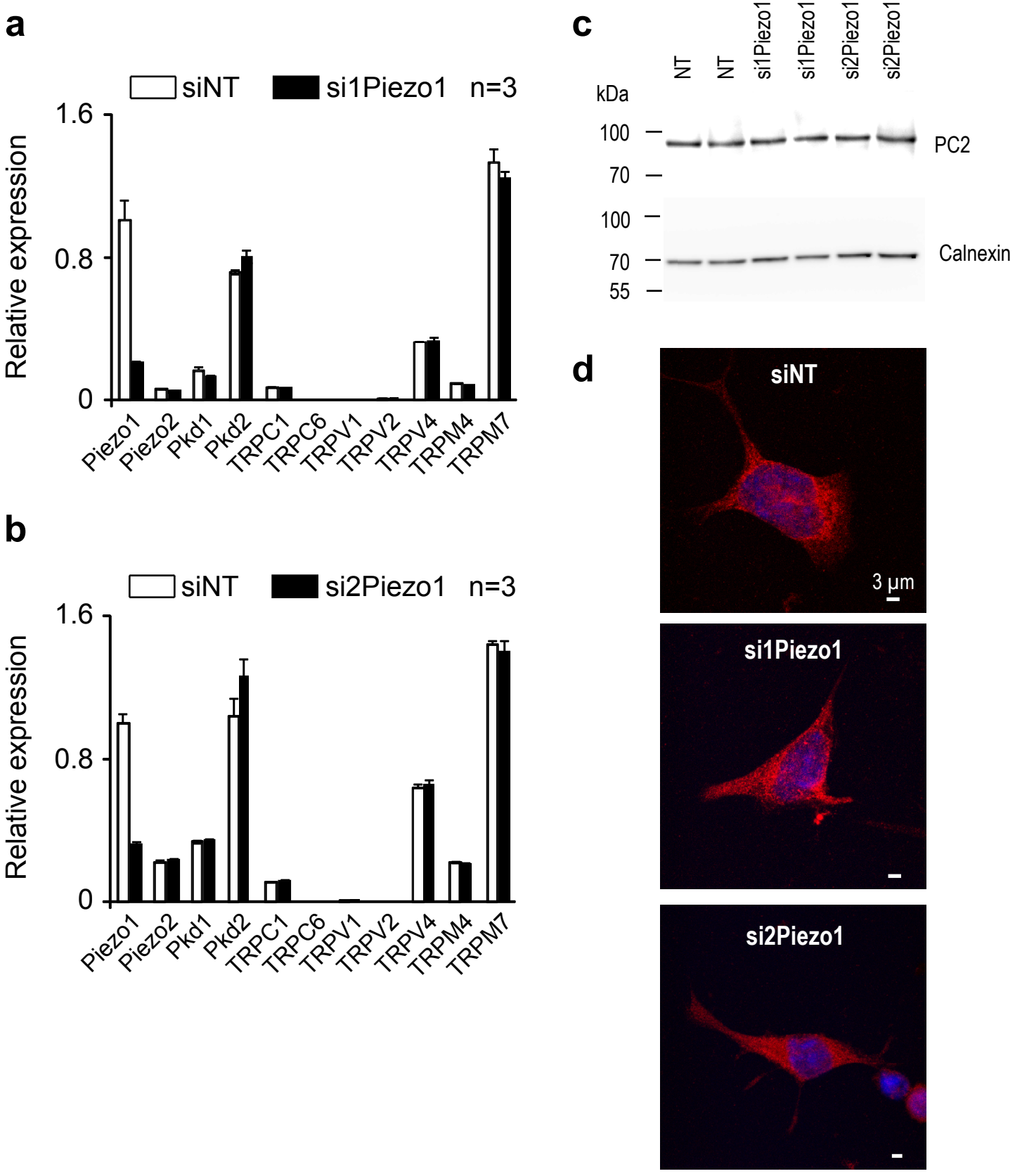

Figure Supp 1

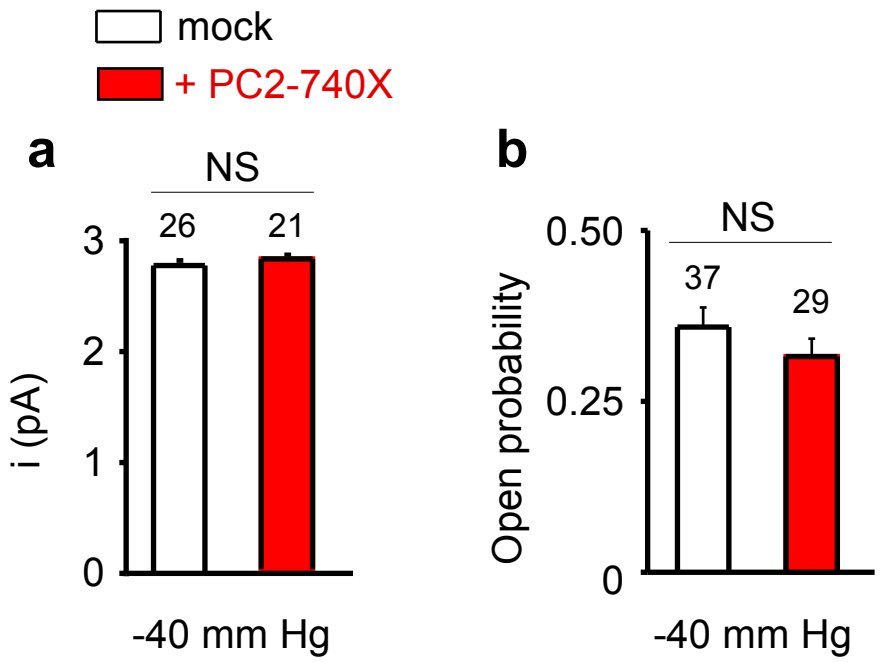

Figure Supp 2

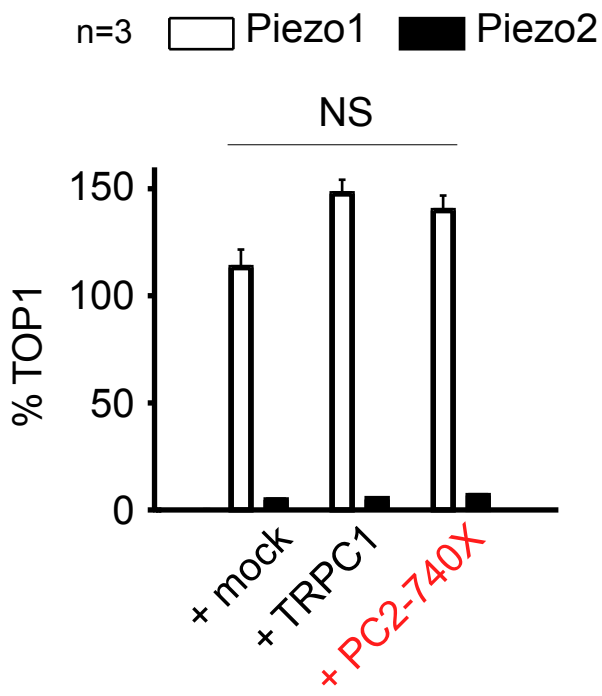

Figure Supp 3

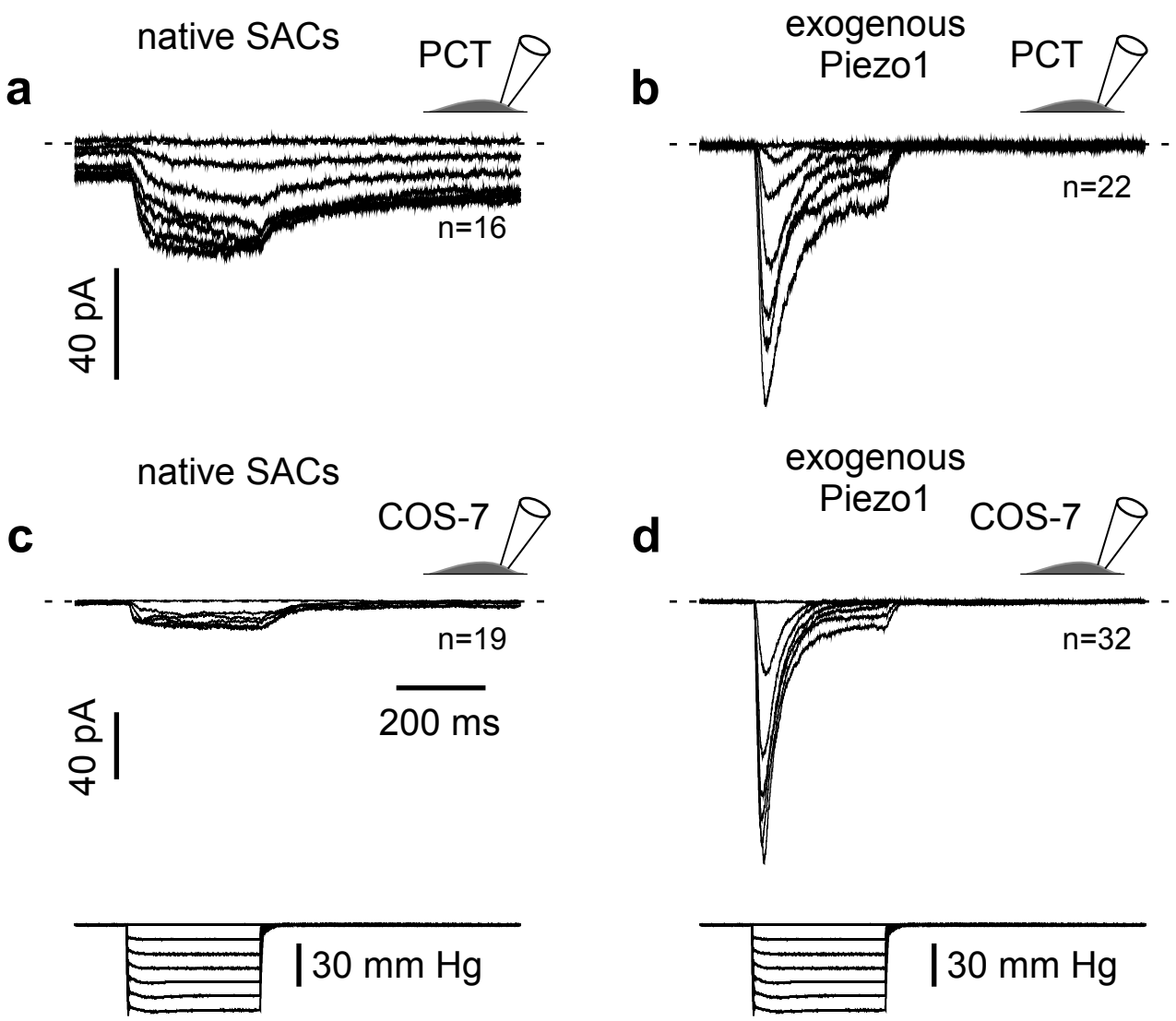

Figure Supp 4

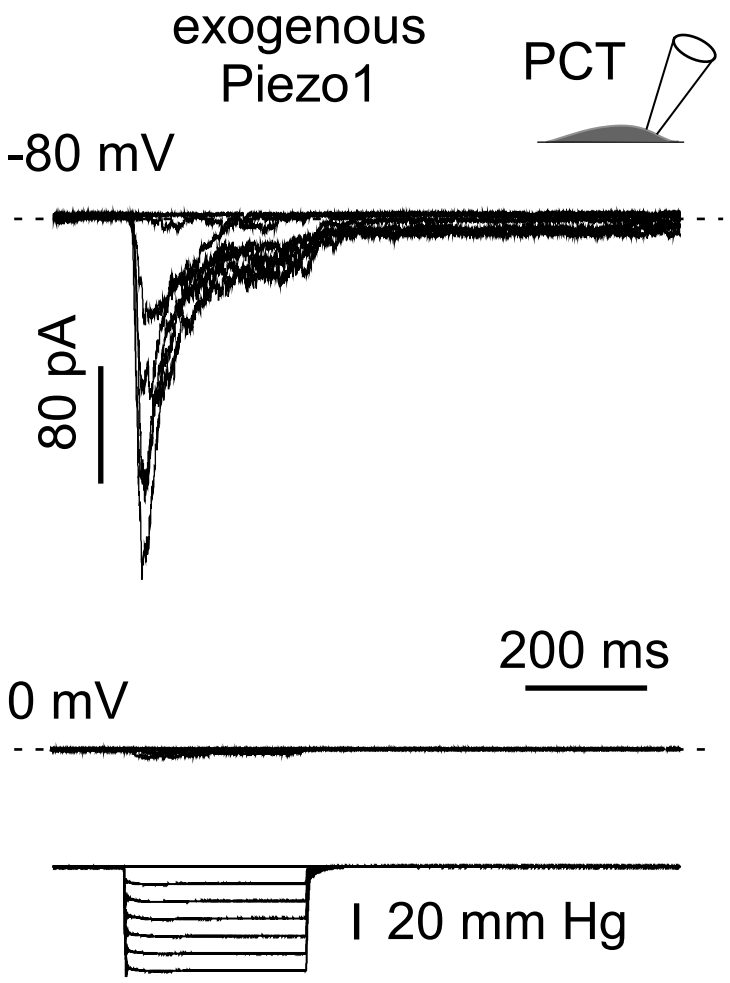

Figure Supp 5

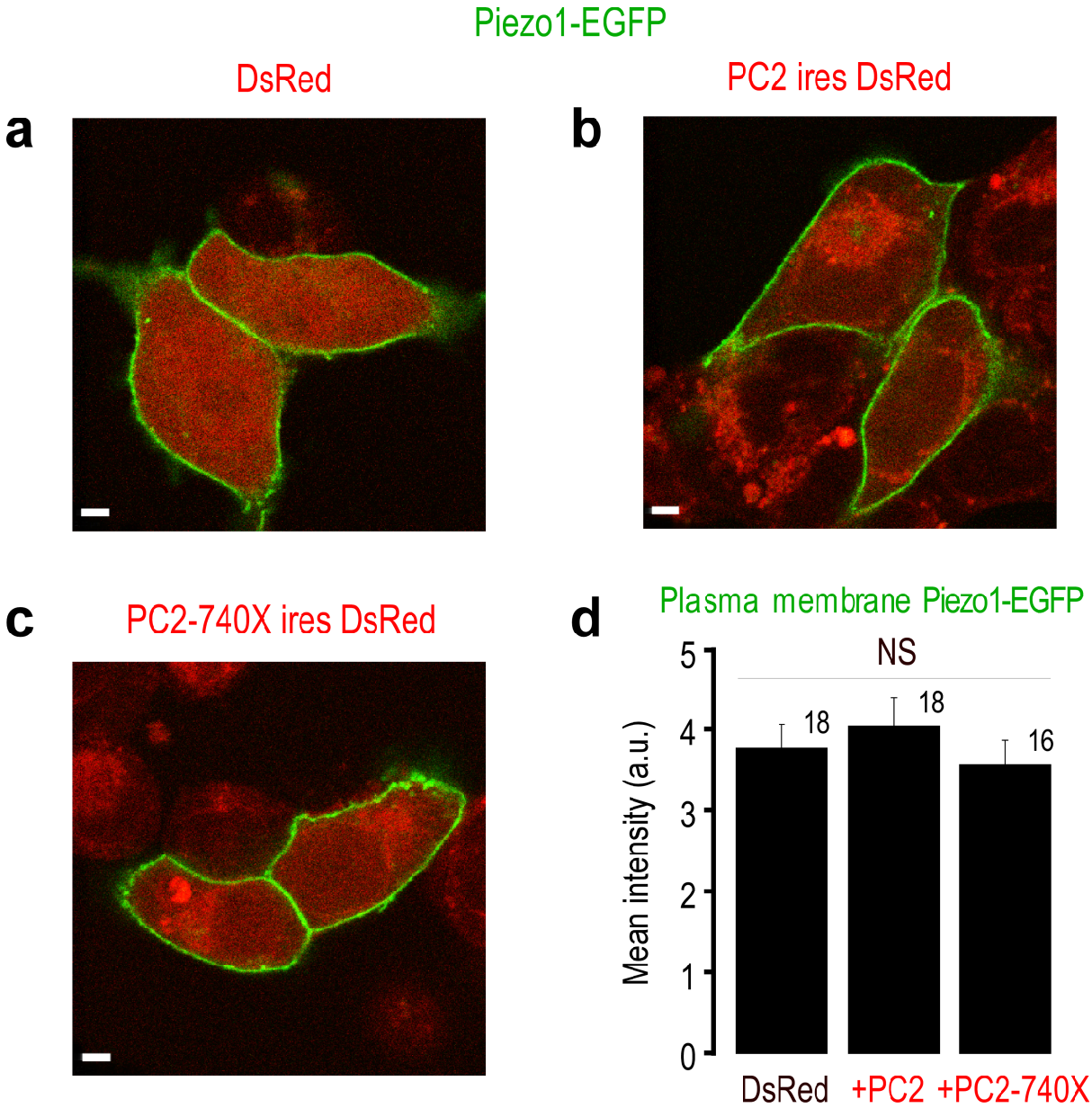

Figure Supp 6

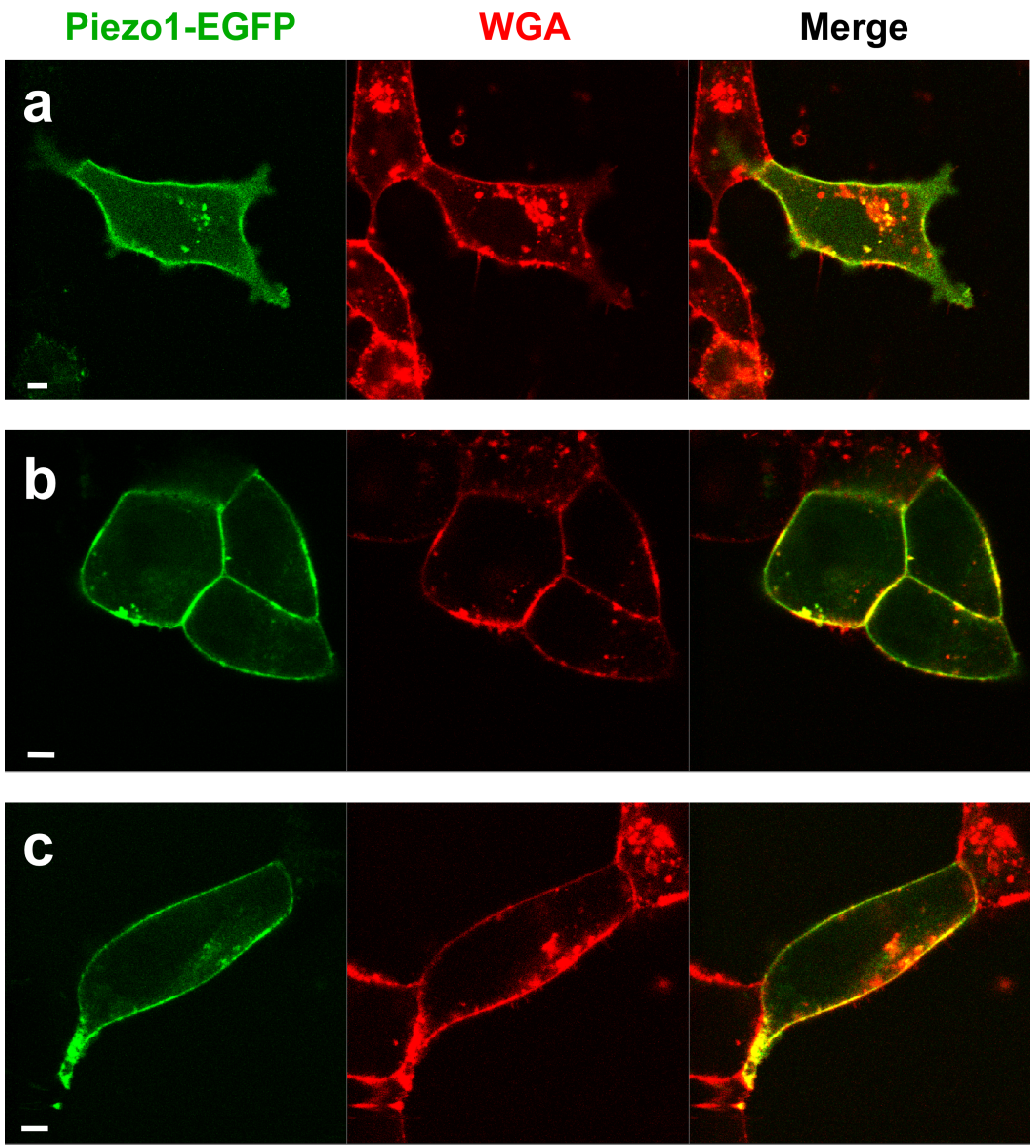

Figure Supp 7

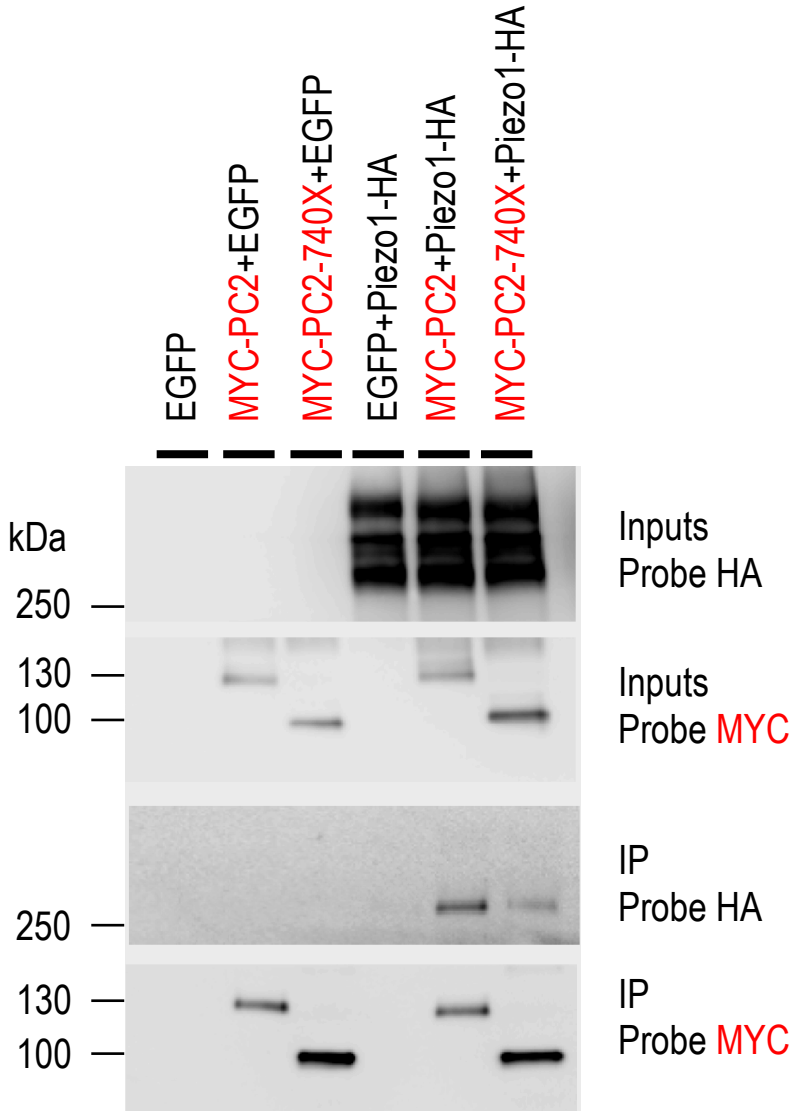

Figure Supp 8

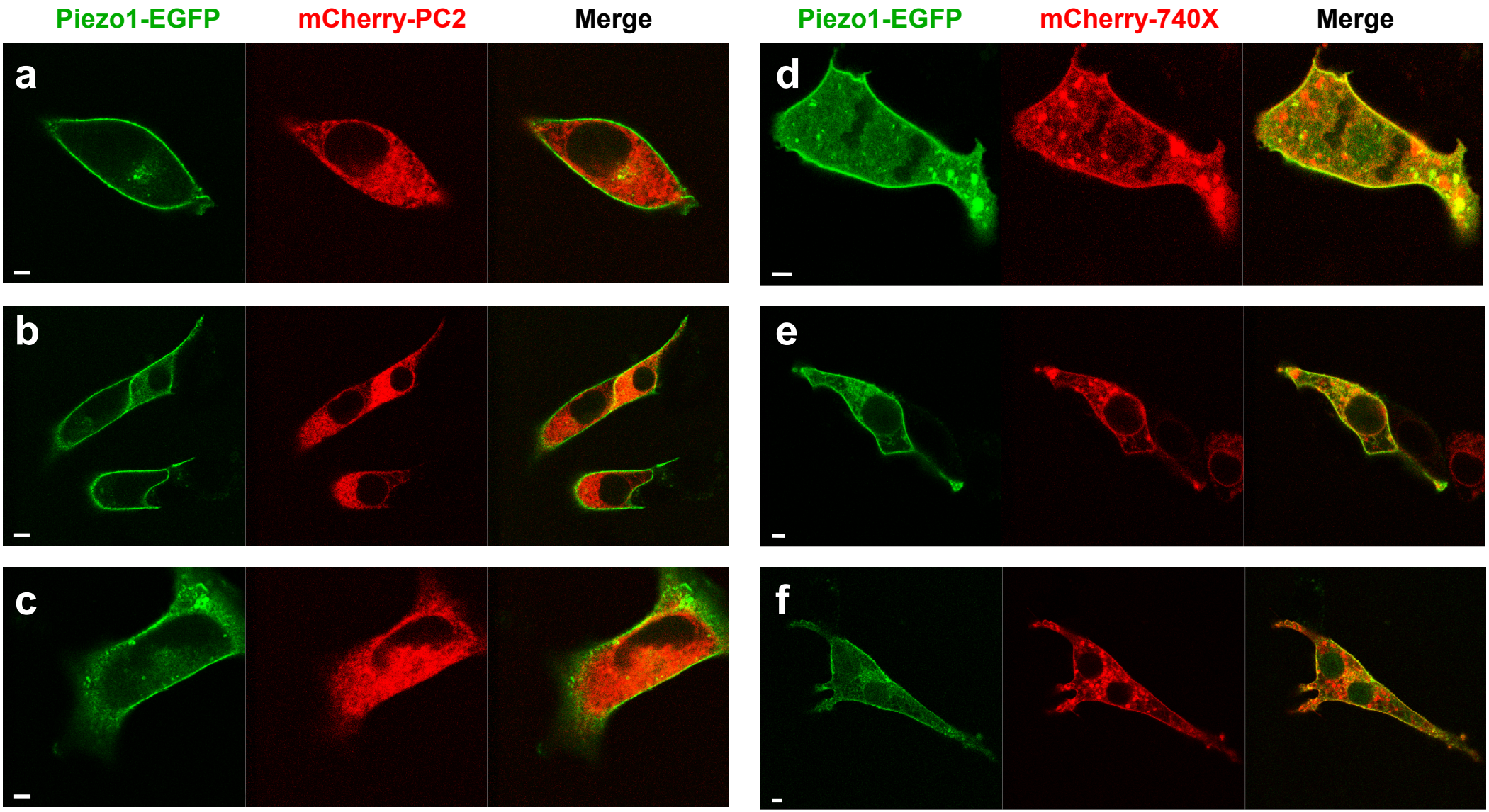

Figure Supp 9